

Flow of lubricated granular material on an inclined plane

Ravindra S. Ghodake^{a,c}, Pankaj Doshi^{b,*}, Ashish V. Orpe^{a,c,*}

^a*Chemical Engineering and Process Development Division, CSIR-National Chemical Laboratory, Pune 411008 India*

^b*Worldwide Research and Development, Pfizer Products India Private Limited, Mumbai 400051 India*

^c*Academy of Scientific and Innovative Research (AcSIR), Ghaziabad 201002 India*

Abstract

We have studied the gravity driven flow of spherical shaped, millimetric sized granular material coated with aspherical, micron-sized, near frictionless lubricant particles. Experiments were performed on an inclined plane using two different sized particles for varying concentrations of the lubricant. The particle volumetric flow rate exhibits a non-monotonic behavior with increasing lubricant concentration. It shows an increase at smaller lubricant concentration followed by a decrease at higher lubricant concentration. The lubricant particles adheres to the granular particle surface thereby reducing the inter-particle friction. However, presence of lubricant particles at higher concentration damps out inter-particle collision thereby reducing the inter-particle momentum transfer. Non-monotonicity in the observed behavior is then conjectured to arise due to competing effects of inter-particle friction and inter-particle collision. The present work and the overall observed behavior therein provides a simple experimental system to characterise the effects of added lubricant material in pharmaceutical and other relevant industrial applications.

Keywords: granular, powder, lubrication, friction, inclined plane

*Corresponding authors

Email addresses: pankaj.doshi@pfizer.com (Pankaj Doshi), av.orpe@ncl.res.in (Ashish V. Orpe)

1. Introduction

Can we simply alter the inter-particle interaction, a fundamental quantity governing the overall behavior in a dry granular system? Doing so essentially will require either some kind of chemistry to alter the particle surface or altering the material itself. Both these methods will change the inter-particle friction and collision characteristics thereby modifying the flow. However, both the methods pose restrictions in terms of material availability and limited scope and ease in use of chemical treatment. Alternatively, DEM simulations allow for studying dry granular systems by suitable tuning of inter-particle friction and collisional properties [1, 2, 3]. But the technique still presents limitations in terms of availability of experimental studies for a detailed comparison in spite of several reported studies [4]

As it turns out, addition of plate-like particles (typically Magnesium Stearate or MgSt) alters the inter-particle interactions in dry systems substantially [5]. This technique is used routinely in pharmaceutical industries handling granular material in various forms. The primary aim is to reduce the friction in the compression die during the process of tablet compaction. As an additional benefit the presence of MgSt also enhances the powder flowability. Typically, the MgSt powder is added in tiny quantities (weight ratio of $O[10^{-2}]$). The individual particles, about 10 micron sized, adhere to the large particles and are expected to reduce the friction between them due to their own frictionless nature thereby enhancing the flowability. This flowability, using MgSt as lubricant, has been studied previously to a reasonable effect [6, 7, 8, 9, 10, 11, 12]. However, all these studies have primarily focused on characterising the optimality in terms of lubricant concentration vis-a-vis flow characteristics. One of them have also focussed on studying the avalanching and angle of repose behavior of pharmaceutical powders in presence of various types of lubricants [10]. It was observed that the addition of lubricant decreases the angle of repose and the time for avalanching. The observed behavior was explained based on particle morphology using scanning electron microscopy (SEM) imaging. On the other hand

usage of powder as a lubricant between two planar solid surfaces is very well known within the domain of tribology and its merits and demerits with respect to conventional liquid lubricants have been well documented [13]. However, the carryover of the flow [14, 15] and rheology [16] characteristics from these planar surface studies to bulk flow of lubricant-granular particles is not known.

Over here we attempt to connect the presence of lubricant particles, their influence on the inter-particle interactions and eventually on the shear flow behavior in terms of flow and concentration profiles using flow visualization techniques. Given that MgSt particles are soft in nature, their excessive presence and effectively higher coating on the larger particles can render the latter to be soft, thereby inducing a higher loss of momentum during collisions. This may effectively nullify the advantage gained due to friction reducing properties of the lubricant. We strive to understand these possible contrasting behaviors in this work through detailed experimentation. To obtain the necessary shear flow, we have chosen chute (inclined plane) system, which is very well studied in literature [4, 17, 1, 18, 2, 19, 20, 21] covering various flow aspects and is, moreover, simple in its handling and usage. The choice of the experimental system is purely incidental and the purpose of this work is not to delve into the details of inclined plane mechanics, but simply to create a shear flow which will allow for studying and understanding the lubricant influence on the flow behavior.

2. Methodology

Experiments are performed on a chute inclined at an angle (θ) as shown in fig. 1. The system comprises two sections. The uppermost section of length 450 mm, width 50 mm and height 400 mm functions as a hopper filled with granular material. The rest of the section, of length 1350 mm, width 50 mm and height 200 mm, functions as a chute. The material from the hopper flows on to the chute through a gap of height 30 mm which can be opened or closed using a manually operated gate. The side walls of the entire system are made

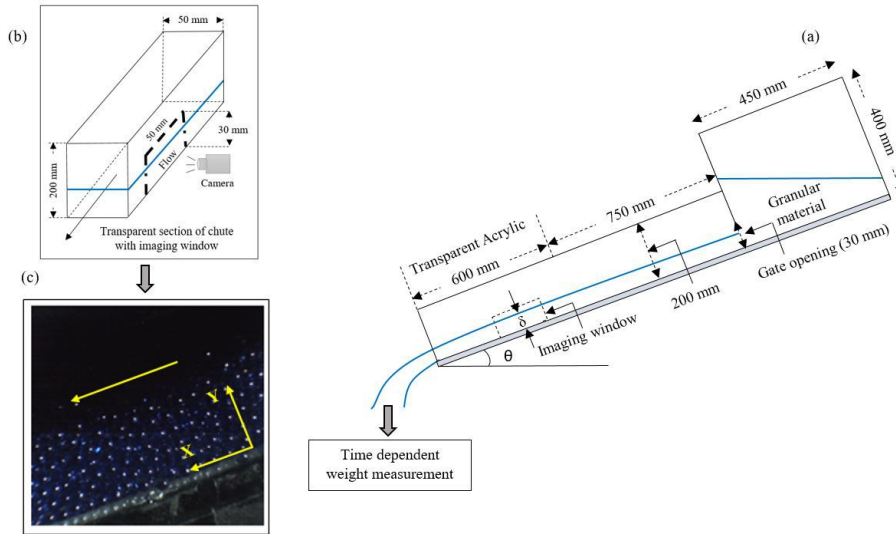


Figure 1: Schematic of the chute flow system. (a) Side view exhibiting hopper, chute, collection system and relevant dimensions. (b) Imaging of the flow at one of the chute side wall (c) Sample image captured using a high speed camera. See text for more details

out of stainless steel (SS316), except for a transparent acrylic window of length 600 mm and height 200 mm, located downstream (600 mm from chute end) for imaging the flow. The base of the chute (of width 50 mm) is made from glass and is roughened by gluing glass beads of desired diameter (d) on it.

Nearly spherical glass beads (Jaygo Inc., USA) of diameter $d = 2$ and 3 mm, with a polydispersity of 15% are used as granular material, while Magnesium Stearate (MgSt) powder (Loba Chemie, India) is used as a lubricant material. The individual particles of MgSt powder have plate-like structure, equivalent sphere volume diameter of $10 \mu\text{m}$ with polydispersity of 10% and are nearly frictionless with respect to each other. For each experiment, a pre-defined, but very tiny, quantity of MgSt powder was mixed with granular beads of either size in a mixer. The mixer comprises an open plastic tank (diameter 185 mm and height 100 mm) fitted with an overhead stirrer. The mixing, for each experiment, was carried out by rotating the stirrer at a speed of 30 revolutions per minute (rpm) over a duration of 5 minutes. The glass beads were colored

using blue ink (Camlin Inc.) for ease in imaging and analysis. The MgSt powder, white in color and slightly cohesive in nature, adheres itself to the surface of the glass beads during the mixing process. The weight ratio of MgSt to glass beads was varied between $O(10^{-5})$ and $O(10^{-3})$ across all experiments. For a given weight ratio, the lubricant concentration was defined $c_l = M_l/A_p$, where M_l is the total mass of lubricant, $A_p = n\pi d^2$ is the total surface area of particles, d is particle diameter and n is the number of particles. The value of n is determined as $(6/\pi d^3)(M_p/\rho_p)$, where M_p is total mass of particles, ρ_p is the particle density ($2.5g/cm^3$) and M_p/ρ_p is the total particle volume.

Given the tiny amounts of added MgSt powder and the small size of individual particles, it was not possible to quantify the homogeneity of mixing as well as any loss of MgSt powder in the mixing vessel. We, thus, resorted to visual inspection, ensuring that the mixed material has whitish appearance and no obvious traces were left on the mixer wall and stirrer surface. To ensure consistency of the mixture, the mixing procedure, including mixing time and speed, was maintained constant across all the experiments. The surface of particles after mixing with lubricant was imaged using FE-SEM (Field Emission Scanning Electron Microscopy) to confirm the altered texture and the adherence of the lubricant. Figure 2 shows the images of 3 mm glass beads at two different magnifications for three different lubricant concentrations. A clean surface is visible in fig. 2b which gets progressively patchy with increasing lubricant concentration as seen in fig. 2d and f. Multiple layers of lubricant are visible at the highest lubricant concentration. Similar surface texture variation is also observed for 2 mm glass beads (not shown).

For every experiment, the chute hopper was filled upto 25% of its total volume with the mixture of glass beads and MgSt while keeping the opening closed. This ensured adequate supply of continuous feed to achieve steady flow for reasonable duration in the experiment. The gate was opened manually to allow gravity induced flow of material down the chute surface. Given that our primary objective was to study the effect of lubricant on the flow and not chute flow mechanics, we kept all the operating parameters constant throughout,

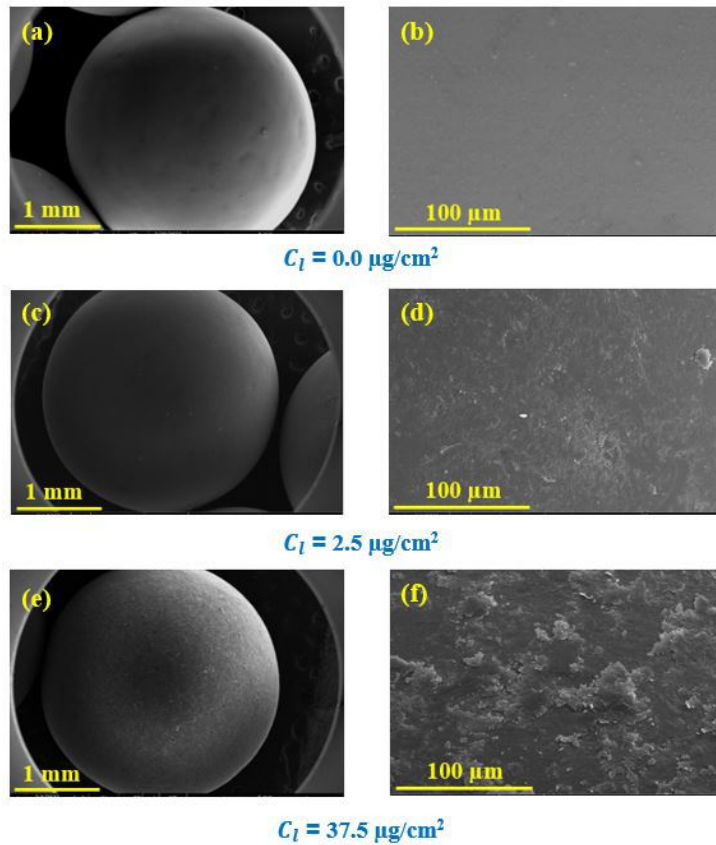


Figure 2: FE-SEM images of individual glass beads of diameter 3 mm after mixing with the lubricant at different concentrations. Images in the right column represent the magnified view of the full particle images shown in the left column. The scales are provided for ready reference. The mixing was carried for 5 minutes using a stirrer speed of 30 rpm.

except for the lubricant concentration being varied for each bead size. The gate was kept in a fully opened state (height 30 mm) across all the experiments. The chute (glass) base was roughened with 2 mm beads for the flow of 2 mm as well as 3 mm glass beads. For a specified chute angle, the material exiting the chute was collected directly on a weighing scale to obtain its time dependent behavior. A small time duration window (4s to 8s) exhibited linear variation of mass collected with time which provided the steady state mass flow rate (m). The chute inclination angle was fixed at 24 degrees and 22 degrees, respectively, for 2 mm and 3 mm glass beads. A progressive increase in the chute angles led to faster flows and consequently reduced time duration of steady state flow. As described next, the higher duration of steady flow rate is desirable for acquiring sufficient number of flow images to get better statistics for time averaged flow velocities. On the other hand, decreasing the angles led to slower flows with increasing probability of flow intermittency. The chute angles specified above were chosen so as to achieve reasonable optimality between flow duration and flow smoothness, which does not necessarily occur at the same angle for both particle sizes.

For the steady state flow duration, images of the flowing glass beads were acquired simultaneously near the side wall in the downstream region using a high speed camera (IDT Y4) (see fig. 1b). The camera was positioned orthogonal to the chute wall and images were taken at 1500 frames per sec over a region of length $30d$ and height $20d$. A typical image of the flowing glass beads from one of the experiment is shown in fig. 1c. The particle centers in each image were obtained using the IDL (Interactive Data Language) centroid algorithm available as open source software [22]. The instantaneous particle velocities in x - y plane were measured from the particle positions in successive images and the time delay between successive positions. Here, “ x - y ” plane represents chute wall, “ x ” represents flow direction and “ y ” represents the direction normal to the flow. The entire flowing layer was divided into horizontal bins of width ($w = 1d$) and length ($l = 20d$), oriented parallel to the chute surface. The velocity (v_x and v_y) for each bin was obtained as an average over all particles located within

the bin and across all images. This resulted in profiles of x -direction and y -direction velocities with distance y from the chute surface. Typically, the number of centroids (i.e. particles) detected per bin per image was about 20 close to the base and decreased rapidly close to the free surface. The free surface location was, then, defined as the bin within which not less than 5 particles were detected per image. The distance of the free surface from the chute base was defined as flowing layer thickness (δ). The particle area fraction (ϕ_a) in the flowing layer was obtained as A_p/A_{box} , where $A_p = n \times \pi d^2/4$, $A_{box} = \delta \times l$ and n is the average number of particles (or centroids) counted per image. Within the visualisation zone itself, images were taken at three different locations in x -direction, about $20d$ apart from each other. The velocity profiles for these three locations were nearly the same suggesting of a fully developed flow. Experiments were performed for two different particle sizes and about 8 to 10 different lubricant concentrations. Each experiment was repeated 4 times to obtain the averages and to ensure repeatability of the results.

3. Results & Discussion

In the following, we discuss various attributes of flowing glass beads on the inclined plane with respect to lubricant concentration. The lubricant concentration (c_l) in each case is reported as amount of lubricant material per unit surface area of particles as described in previous section. This, then, correctly accounts for the total area available for the lubricant for both particle sizes considered. The variation of the steady state volumetric flow rate (Q) with lubricant concentration is shown in fig. 3. The volumetric flow rate was obtained by dividing the mass flow rate with particle density ($\rho_p = 2.5 \text{ g/cm}^3$). The data in fig. 3a exhibits several interesting features which we dwell upon in the following.

Typically, the flow rate on an inclined plane, for a fixed particle type, is uniquely determined by the inclination angle and inlet gate opening[17], both of which are maintained constant over here for each particle size considered. However, a spectrum of steady flow rate values, instead of one unique value, is

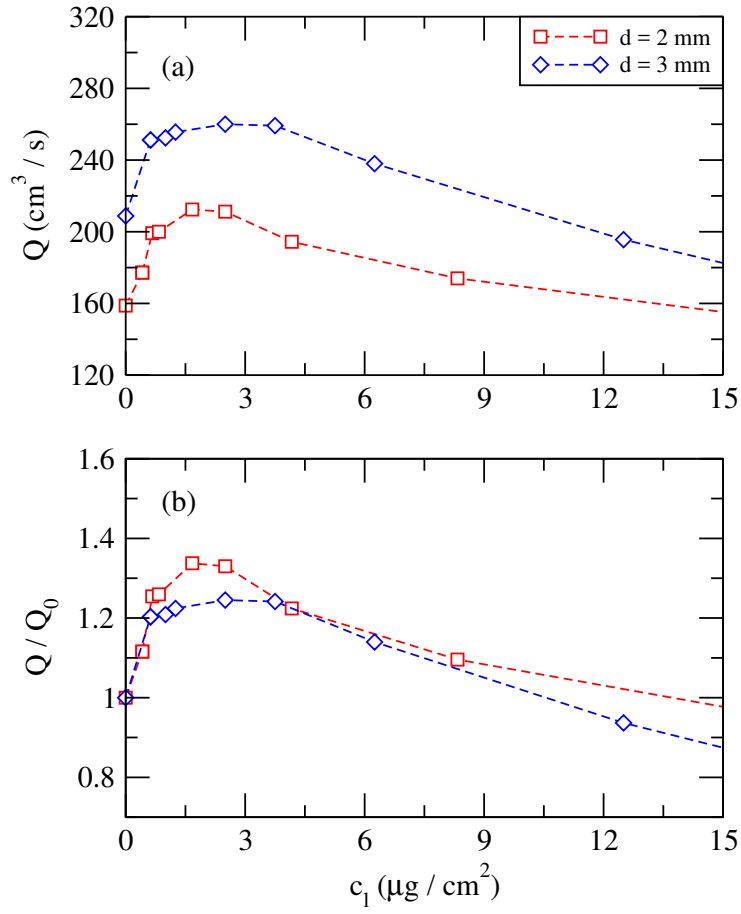


Figure 3: Variation of the volumetric flow rate with lubricant concentration (c_l). (a) Actual values of flow rate (Q) and (b) Values of flow rate (Q) normalised by its value (Q_0) in the absence of lubricant. Chute angle was maintained at 24 degrees and 22 degrees, respectively, for flow of 2 mm and 3 mm diameter glass beads.

observed for each particle. This suggests of the change in the nature of the particle surface with varying lubricant concentration. The lubricant concentration then, possibly, acts as a parameter allowing for studying the effect of particle surface characteristics on the flow behavior. For a given particle size, the flow rate exhibits a non-monotonic dependence on the lubricant concentration. It first increases rapidly for small enough values of c_l followed by a slow decrease over a much wider range of c_l . The presence of a maximum, however, suggests that there exists an upper limit for improving the flowability of glass beads by use of lubricant. The particle surface characteristics which are conducive to higher flowability at lower c_l values seem to get altered at higher c_l values thereby increasing the flow hindrance instead. For very large enough values of c_l , the flow rate value dips below that for base case suggesting that the presence of lubricant actually worsens the flowability. This behavior indicates the presence of two competing effects, the dominance of either varies at different lubricant contents. The maximum value of the flowrate is attained at nearly same value of c_l for all particle sizes, which is not quite surprising considering the surface area driven behavior.

Figure 3b shows variation of normalised volumetric flow rate (Q/Q_0) with lubricant concentration, where Q_0 is the flow rate in the absence of lubricant. The data shows similar behavior and features observed in fig. 3a. The profiles in fig. 3b suggests that the observed non-monotonic dependence due to addition of lubricant can be expected to be generally applicable for various system and operational parameters.

Before focusing on detailed flow characteristics, we first discuss the qualitative nature of the flow as visualised through camera imaging. Figure 4 shows images for three different lubricant concentrations and both particle sizes. In every image the visible base is approximately 8 particle diameters long. The images in the middle column correspond to the lubricant concentration when the flow rate is maximum. The images in the left and right column, respectively, represent the flow in the absence of lubricant and highest lubricant concentration. Sequence of several such images, for every particle size and c_l values, were

used to obtain velocity data presented later on. The images clearly show a qualitative change for varying lubricant concentration. The flowing layer thickness increases for $c_l = 2.5 \mu\text{g}/\text{cm}^2$ than that in the absence of lubricant. The flowing layer appears expanded and seems to be in a fluidized state with particles packed thinly compared to the base case. This leads to a larger flowing layer thickness. The exact opposite behavior is seen for largest value of c_l . The layer appears to be much more densely packed, even more than that for the base case and the thickness is reduced. Thus, the non-monotony observed earlier for flowrate, seems to be preserved for packing fraction as well as layer thickness. More details of the flow behavior for all the cases shown in fig. 4 can be seen in the movies provided as Supplemental material. As evidenced from the movies, the flow slows down substantially for the highest value of c_l , while it is much faster for intermediate value of c_l . The behavior then follows the classical Reynolds dilatancy theorem which states that the material has to dilate to flow faster (see fig. 4).

The volumetric flow rate can be expressed as $Q = u\delta\phi_v W$, where u is the mean velocity in the flowing layer, W is the flowing layer width, δ is the flowing layer thickness and ϕ_v is the mean particle volume fraction in the flowing layer. Given that W is maintained constant, the flow rate variation will be governed by changes in the remaining three variables for various lubricant concentrations. Since all the measurements were carried out near the side walls, we report variation of particle area fraction (ϕ_a) in the following instead of volume fraction (ϕ_v). The flow direction velocities (v_x) were averaged across the entire flowing layer thickness (δ) after subtracting the slip velocity (v_s) at the chute base to obtain the depth averaged mean velocity (u) in the flowing layer. The variation of the mean velocity (u), with lubricant concentration is shown in fig. 5a. The mean velocity variation nearly mimics the trend for the volumetric flow rate shown in fig. 3. It increases rapidly for small enough values of c_l and then decreases slowly over larger values of c_l , with a maximum at an intermediate value of c_l . On the other hand, the layer thickness (δ) for both particle sizes shows an increase for lower values of c_l and it almost remains constant at higher

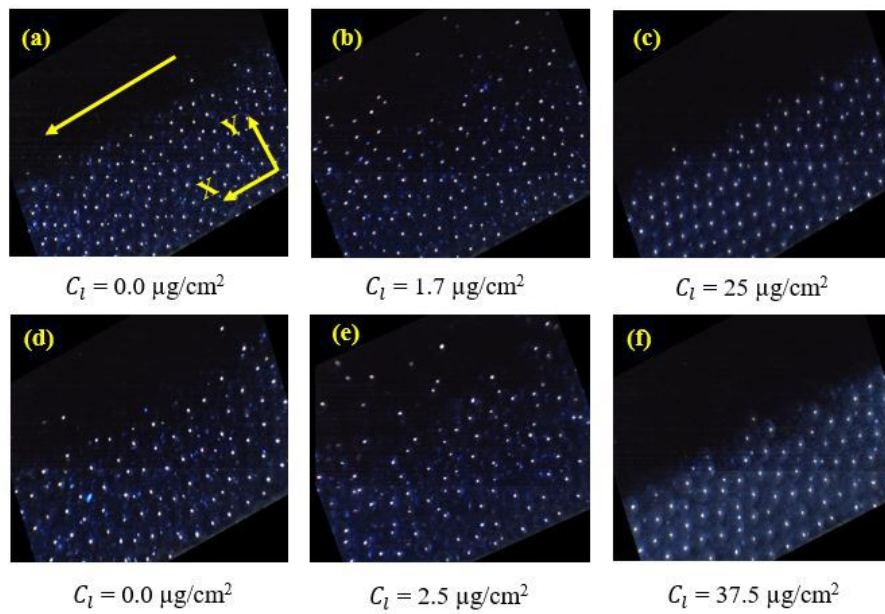


Figure 4: Images of the flowing layer of glass beads for different lubricant concentrations. Upper row and lower row, respectively, represent images for 2 mm and 3 mm diameter glass beads. Chute angle was maintained at 24 degrees and 22 degrees, respectively, for flow of 2 mm and 3 mm diameter glass beads.

values of lubricant concentration (see fig. 5b). Consequently, the area fraction (ϕ_a) shows rapid decrease for lower c_l values before increasing at higher values of lubricant concentration (see fig. 5c). These behaviors of layer thickness and area fractions are quantitative representations of what is observed in fig. 4.

The lubricant (MgSt) particles are cohesive in nature and on mixing adhere to the surface of the glass beads (see fig. 2). The magnified images show that the lubricant particle coats the glass beads in patches which seem to increase in size and thickness at very large concentrations. Given their nearly frictionless nature, the lubricant (MgSt) particles on adhering to the glass beads are expected to reduce the friction coefficient between glass beads at contact. The increase in the flow rate can, then, be attributed to a decrease in the average inter-particle friction coefficient, leading to a faster flow direction velocity. This leads to enhanced collisions accompanied by lesser dissipation of particle kinetic energy causing expansion of the flowing layer. We allude to average value of friction over here, given that not all particles can be coated equally by the lubricant and also not every inter-particle contact will have lubricant presence. For large enough concentrations, the glass beads get coated by the lubricant particles (see figs. 2f). While this additional coating cannot be expected to further reduce inter-particle friction, it can very well increase the dissipation during particle collisions, thereby slowing down the flow while nullifying any advantage due to reduced friction. Note that the lubricant particles are also quite soft (malleable) in nature. The increased dissipation also leads to flowing layer contraction. While this dissipation due to inter-particle collision exists for all values of c_l , its effect seems to get more pronounced with increasing lubricant concentration. The non-monotonic behavior in that case can be considered to arise due to competing effects of inter-particle friction and collision, leading to a maximum at intermediate values of c_l . The damping effect progressively increases such that at highest concentration studied the flow rate reduces than the base case value. With further increase in the value of c_l , the flow can be expected to cease completely due to excessive inter-particle damping.

The presence of lubricant also seems to induce microstructural changes in

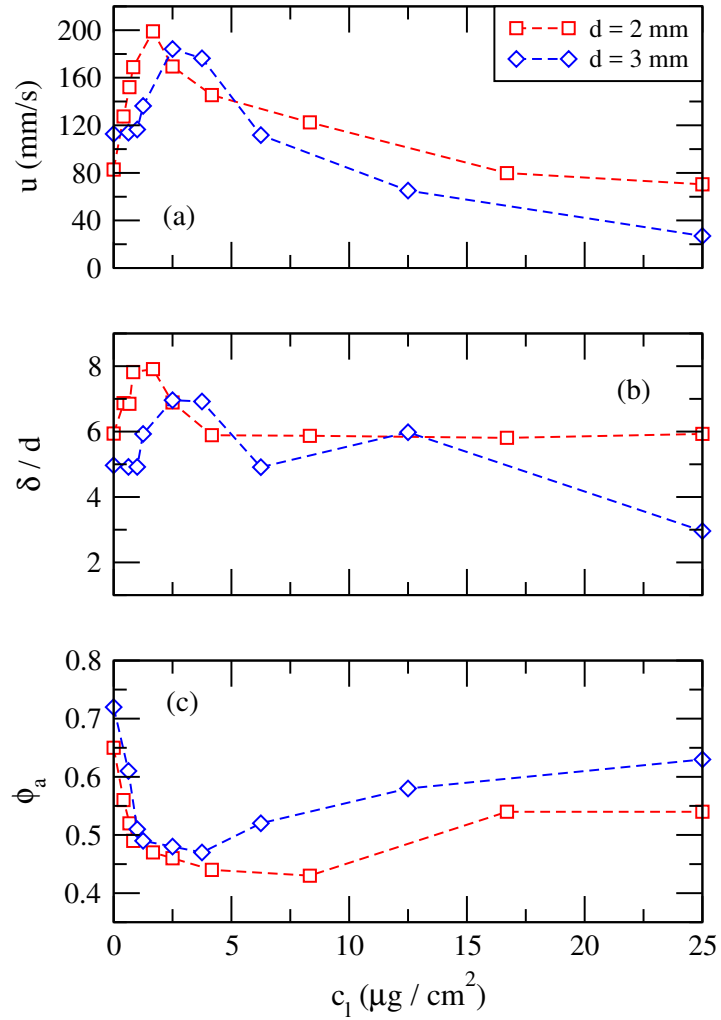


Figure 5: Variation of (a) flow depth average velocity (u) of particles in the flowing layer (b) flowing layer thickness (δ/d) and (c) area fraction (ϕ_a) measured near the walls with lubricant concentration (c_l). Chute angle was maintained at 24 degrees and 22 degrees, respectively, for flow of 2 mm and 3 mm diameter glass beads.

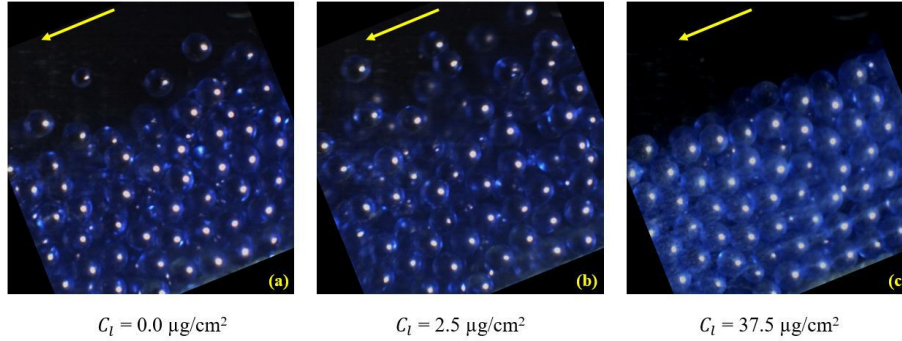


Figure 6: Magnified images of the flowing layer of 3 mm diameter glass beads for different lubricant concentrations showcasing the state of particle packing. Chute angle was maintained at 22 degrees.

the flowing layer giving rise to varying degree of compactness which is quantified in fig. 5c and visualised through magnified images shown for 3 mm diameter glass beads in fig. 6. Similar behavior is also observed for 2 mm glass beads (not shown). For the base case, i.e. in the absence of lubricant, the layer shows reasonable packing particularly in the few layers near the base. The layer seems to comprise separate clusters of few particles throughout without connectivity across the entire layer. For intermediate lubricant concentration (see fig. 6b), the flowing layer expands and the interconnectivity between the beads is diminished even further. The flowing layer, in this case, is dominated by inter-particle collisions. For the highest lubricant concentration studied, the flowing layer compacts substantially with significant connectivity lasting over several beads instead of few clusters as evident for lesser lubricant concentrations. Moreover, the flowing layers shows the beads arranged in layers which move over one another (see movie provided as supplementary material), not quite evident at lesser lubricant concentrations. We conjecture that this compaction and layering arises due to enhanced damping during collisions at higher lubricant concentrations. While it cannot be ascertained quantitatively, the layering may be associated with load bearing stress chains spanning across the layer which may govern the overall flow behavior.

The above alluded interactions are not feasible to be measured at individual particle level given that the actual interactions can be between two or more particles. Further, it may not provide reasonable insight given the variation in the lubricant coating across several glass beads. Since all the observations are made at the flow (bulk) scale it is necessary to determine the quantity that can describe the bulk behavior appropriately. This quantity will, then, represent an effective or an average of actual interactions occurring at the individual particle level, but manifested at the bulk level.

To quantify the effective (or average) interactions between lubricant coated glass beads we measure the static angle of repose (θ_r). To carry out these measurements we slowly pour mixture of glass beads and lubricant of various concentrations in a rectangular cell of height (21 cm), length (48 cm) and width (3.5 cm) to form a static heap. The length and height are sufficiently large so as to prevent any kind of end effects. The static image of the heap was captured using a digital camera positioned sideways and orthogonal to the side wall of the rectangular cell. Central, nearly flat, free surface, region of the heap (about 20 cm long) was analysed to obtain the angle of repose. Every experiment was carried out 6 times to ensure repeatability. Note that the tangent of the angle of repose ($\tan \theta_r$) can be considered as the effective friction coefficient. We conjecture that this angle should be the result of interactions spanning several particles and is an inherent property of the material. In essence, it should capture the countering effects of varying inter-particle friction and inter-particle damping.

The variation of the static angle of repose (θ_r) with lubricant concentration is shown in fig. 7. The observed behavior correctly captures the flow rate and velocity curves with respect to lubricant concentration. The static angle of repose (i.e. effective friction coefficient) also shows a non-monotonic dependence on lubricant concentration (c_l) with the location of minimum at same value of c_l for both particle sizes. For small enough lubricant concentrations, the value of θ_r progressively decreases and reaches a minimum. This indicates that the heap of material flows relatively easily and settles at a lower angle of repose.

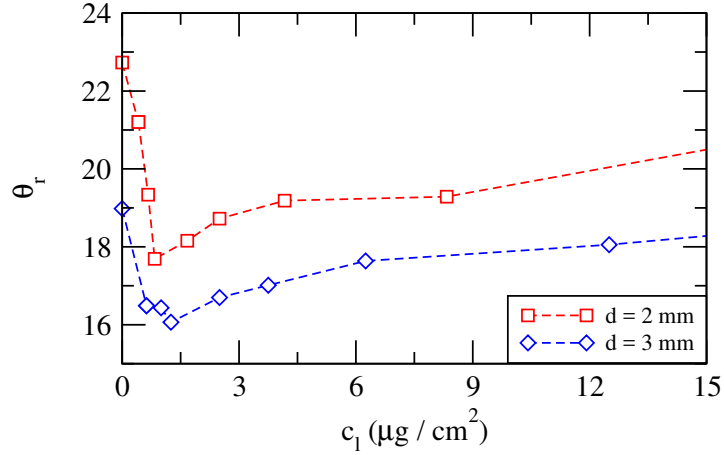


Figure 7: Variation of static angle of repose (θ_r) with lubricant concentration (c_l) for the two particle sizes.

Correspondingly, the material progressively flows faster on the chute surface leading to the increasing part of the flow rate (see fig. 3) and velocity curves (see fig. 5a). However, for large enough concentrations, the flowability progressively reduces with pile settling at higher angles. This behavior seems more likely to arise due to increased damping of softer, highly coated glass beads rather than increased inter-particle friction. Not surprisingly, flow rate and mean velocity curves show a progressive decrease at larger lubricant concentrations. In fact for large enough values of c_l , the flow rate reduces below the base case value (in absence of lubricant). It can, thus, be expected that the flow will completely cease to stop at very high lubricant concentrations with the value of angle of repose (from heap measurements) more than the inclination angle of the chute. Similar qualitative behavior the angle of repose was also previously observed by Morin and Briens [10] for various types of lubricants. The study showed that the angle of repose decreased to a lower value for smaller lubricant concentrations, but unlike the observations over here, it stayed nearly at the same value for even higher lubricant concentrations. We attribute these differences to the type of granular particles (very small sized, cohesive pharmaceutical powders) used

in the work as against large sized, non-cohesive glass beads used over here.

4. Summary

In summary, we have investigated the flow behavior of granular material in the presence of a tiny amount of very small sized Magnesium Stearate as lubricant particles. The overall behavior shows a distinct non-monotonic dependence on increasing concentration of the lubricant particles. For small enough lubricant concentrations, the particles move much faster while at very large concentrations, the flow slows down substantially. The maximum value is obtained for the same value of lubricant per unit particle surface area for different sized particles. The observed non-monotonic behavior is explained through measurement of static angle of repose which represents effective friction. We conjecture that the measured effective friction is realised because of competing effects between (i) reduced inter-particle friction due to frictionless lubricant adhering to the particle surface and (ii) damping due to excessive coating of lubricant on the particle surface thereby rendering them softer. The latter effect is typically not observed in pharmaceutical powders, but seems to be a signature of the hard-sphere like, non-cohesive, large sized granular particles used over here. For such particles the normal interaction (or collisions) do contribute substantially to the overall flow behavior in addition to inter-particle friction. Nevertheless, the inclined plane geometry used in this work do seem to provide an alternative, simpler system to those typically used in pharmaceutical powder flow characterisation. It, however, remains to be seen if the observed behavior over here carries over smoothly to the cohesive, pharmaceutical, small sized fine powders.

Acknowledgements

AVO gratefully acknowledges the financial support from Science & Engineering Research Board, India (Grant No. CRG/2019/000423).

Supplementary data

The supplementary material (movie files and their information) related to this article are also uploaded to arXiv.

References

References

- [1] L. E. Silbert, D. Ertas, G. S. Grest, T. C. Halsey, D. Levine, S. J. Plimpton, Granular flow down an inclined plane: Bagnold scaling and rheology, *Phys. Rev. E* 64 (2001) 051302-1.
- [2] L. E. Silbert, J. W. Landry, G. S. Grest, Granular flow down a rough inclined plane: Transition between thin and thick piles, *Phys. Fluids* 15 (2003) 1.
- [3] A. V. Orpe, P. Doshi, Friction-mediated flow and jamming in a two-dimensional silo with two exit orifices, *Phys. Rev. E* 100 (2019) 012901.
- [4] G. Midi, On dense granular flows, *Eur. Phys. J. E* 14 (2004) 341.
- [5] C. C. Sun, Decoding powder tabletability: Roles of particle adhesion and plasticity, *J. Adhes. Sci. Technol.* 25 (2011) 483.
- [6] M. Llusa, F. J. Muzzio, The effect of shear mixing on the blending of cohesive lubricants and drugs, *Pharm. Technol.*
- [7] C. V. Navaneethan, S. Missaghi, R. Fassihi, Application of powder rheometer to determine powder flow properties and lubrication efficiency of pharmaceutical particulate systems, *AAPS PharmSciTech* 6-3 (2005) E398.
- [8] J. K. IV, F. Moore, Scale-up model describing the impact of lubrication on tablet tensile strength, *International Journal of Pharmaceutics* 399 (2010) 19.

- [9] S. Lakio, B. Vajna, I. Farkas, H. Salokangas, G. Marosi, J. Yliruusi, Challenges in detecting magnesium stearate distribution in tablets, *AAPS PharmSciTech* 14 (2013) 435.
- [10] G. Morin, L. Briens, The effect of lubricants on powder flowability for pharmaceutical application, *AAPS PharmSciTech* 14 (2013) 1158.
- [11] Y. Wang, J. G. Osorio, T. Li, , F. J. Muzzio, Controlled shear system and resonant acoustic mixing: Effects on lubrication and flow properties of pharmaceutical blends, *Powder Technology* 322 (2017) 332.
- [12] W. R. Ketterhagen, M. P. Mullarney, J. Kresevic, D. Blackwood, Computational approaches to predict the effect of shear during processing of lubricated pharmaceutical blends, *Powder Technology* 335 (2018) 427.
- [13] E. Y. A. Worniyoh, V. K. Jasti, C. F. Higgs, A review of dry particulate lubrication, *Trans. ASME J. Tribology* 129 (2007) 438.
- [14] N. Fillot, I. Iordanoff, Y. Berthier, Simulation of wear through mass balance in dry contact, *ASME J. Tribol.* 127 (2005) 230–237.
- [15] I. Iordanoff, B. Steve, Y. Berthier, Solid third body analysis using a discrete approach: Influence of adhesion and particle size on macroscopic properties, *ASME J. Tribol.* 124 (2002) 530–538.
- [16] E. Worniyoh, C. F. Higgs, Self-replenishing, self-repairing solid lubrication: Modeling and experimentation, *Proc. World Tribol. Conf.* (2005) 409–410.
- [17] O. Pouliquen, Scaling laws in granular flows down rough inclined planes, *Phys. Fluids* 11 (1999) 542.
- [18] P. Jop, Y. Forterre, O. Pouliquen, A constitutive law for dense granular flows, *Nature* 441 (2006) 727.
- [19] P. Mills, D. Loggia, M. Tixier, Model for a stationary granular flow along an inclined wall, *Eur. Phys. Lett.* 45 (1999) 733.

- [20] C. Cassar, M. Nicolas, O. Pouliquen, Submarine granular flows down inclined planes, *Phys. Fluids* 17 (2005) 103301–1.
- [21] C. S. Campbell, C. E. Brennen, Chute flows of granular material: Some computer simulations, *Trans. ASME J. Appl. Mech.* 52 (1985) 172.
- [22] Idl centroid detection algorithm, (<http://www.physics.emory.edu/faculty/weeks/idl/>).